






Demonstration of a High-Efficiency Short-Cavity III-V-on-Si C-Band DFB Laser Diode

Javad Rahimi , Joris Van Kerrebrouck , Bahawal Haq, Johan Bauwelinck , *Senior Member, IEEE*,
Gunther Roelkens , *Senior Member, IEEE*, and Geert Morthier , *Senior Member, IEEE*

Abstract—In this paper we demonstrate a high wall-plug efficiency and low threshold current for heterogeneously integrated III-V-on-Silicon distributed feedback (DFB) lasers. Above 12% wall plug efficiency is achieved for a 200 μm long DFB laser diode at 25 °C. Up to two times 6 mW of optical power is coupled into the silicon waveguide and more than 40 dB side-mode suppression ratio is obtained. We also discuss the non-return-to-zero on-off keying modulation at 20 Gb/s and the transmission over a 2 km long optical fiber.

Index Terms—Heterogeneous integration, direct modulation, distributed feedback lasers, wall-plug efficiency.

I. INTRODUCTION

AS SILICON photonics is penetrating in different market segments, efficient heterogeneously integrated light sources are desirable. Especially in the context of datacom, wall-plug efficiency is critical. In addition, small footprint integrated transmitters have attracted much attention to decrease the final package size and cost of the transceivers [1], [2]. Heterogeneous integration of III-V semiconductors on a silicon-on-insulator (SOI) wafer provides a solution to combine the best of both worlds. In this approach, the III-V material can be first bonded and then processed into active components such as lasers or it can be first processed on its own III-V substrate as coupons and then micro-transfer-printed to the pre-patterned SOI circuits [3], [4]. In recent years, there have been dedicated efforts either in academia or industry to improve the performance of various light sources on Si [5]–[7]. Among the demonstrated integrated light sources, edge emitting laser diodes such as distributed feedback (DFB) lasers or distributed Bragg reflector (DBR) lasers are the transmitter of choice when

fabricating low-cost integrated transmitters for O-band and C-band wavelength division multiplexing (WDM) systems. In addition, they exhibit high modulation bandwidth and output power.

In order to improve the performance of these integrated lasers, the optical mode inside the cavity has to be engineered. Since the III-V material is highly absorbing due to the intervalence band absorption [8], [9], pushing down the hybrid mode into the Si waveguide can result in a reduction of the internal loss and an increase in internal efficiency. On the other hand, the resulting decrease of the optical confinement in the active region can increase the threshold current and degrade the modulation bandwidth. Considering this trade-off in designing the laser cavity, there have been several demonstrations on improving the efficiency and performance of heterogeneously integrated DFB lasers in recent years. In [10], a III-V-on-silicon DFB laser based on adhesive bonding with a wall-plug efficiency of about 9% has been achieved at room temperature considering the output power of both facets. The reported DFB laser structure is based on a 680 μm long quarter-wave shifted second-order grating. In order to couple the light to the silicon waveguide underneath, two 185 μm long spot-size converters are incorporated at both ends of the cavity. [11], [12] demonstrated high modulation speed of III-V-on-silicon lasers with large confinement factor in the III-V active region with both direct and electroabsorption modulation approaches. Low-threshold short-cavity DFB hybrid silicon lasers fabricated with a low temperature molecular bonding process have been reported in [13], [14]. Wall-plug efficiencies up to 3% and 2% were achieved at 1 mW output power for the 100 μm and 200 μm long lasers, respectively [14]. Similar work [15] demonstrated other improvements on III-V-on-silicon C-band DFB lasers, the summary of which can be found in Table I.

Characterization of a heterogeneously integrated DFB laser operating at O-band is demonstrated by Intel in [16]. Lasing is reported up to 150 °C and a wall-plug efficiency of 15% is achieved at 80 °C. However, direct modulation has not been demonstrated with these devices.

To achieve a short cavity length with a large confinement factor in the active region, a combination of direct bonding and epitaxial regrowth has been applied for fabricating membrane lasers on a SiO₂/Si substrate [17]. High performance either in terms of power consumption or modulation bandwidth has been achieved, but at the expense of more complex fabrication [18], [19].

Manuscript received August 4, 2021; revised October 18, 2021 and October 20, 2021; accepted October 20, 2021. Date of publication October 26, 2021; date of current version November 9, 2021. This work was supported by the Methusalem program of the Flemish government. (*Corresponding author: Javad Rahimi.*)

Javad Rahimi, Gunther Roelkens, and Geert Morthier are with the Department of Information Technology (INTEC), Photonics Research Group, Ghent University-IMEC, 9052 Ghent, Belgium (e-mail: javad.rahimi@ugent.be; gunther.roelkens@ugent.be; geert.morthier@ugent.be).

Joris Van Kerrebrouck and Johan Bauwelinck are with the Department of Information Technology (INTEC), IDLab, Ghent University-IMEC, 9052 Ghent, Belgium (e-mail: joris.vankerrebrouck@ugent.be; johan.bauwelinck@ugent.be).

Bahawal Haq is with GlobalFoundries, Dresden 01109, Germany (e-mail: bahawal.haq@ugent.be).

Color versions of one or more figures in this article are available at <https://doi.org/10.1109/JSTQE.2021.3122552>.

Digital Object Identifier 10.1109/JSTQE.2021.3122552

TABLE I
STATIC AND DYNAMIC CHARACTERISTICS OF III-V-ON-SOI C-BAND DFB LASERS

Group	Cavity length (μm)	Threshold Current (mA)	Maximum W.P.E (%)	Maximum on-chip output power (mW)	Slope Efficiency (WA^{-1})	SMSR (dB)	Direct Modulation speed (Gbit/s)	Year	Ref.
Ghent University-IMEC	680	35	9	14	0.135	50	–	2013	[10]
UCSB	200	8.8	>3	>7	≈ 0.1	>55	12.5 @ 62 mA	2014	[14]
UCSB	400	7.5	≈ 3	>5	≈ 0.06	>55	–	2016	[13]
Ghent University-IMEC	340	32	≈ 3.3	>7	0.072	45	56 @ 110 mA	2017	[11]
III-V Lab	600	35	–	–	0.12	>50	32 @ 100 mA	2018	[15]
This work	200	10.5	12	>12	0.185	44	20 @ 70 mA	2021	

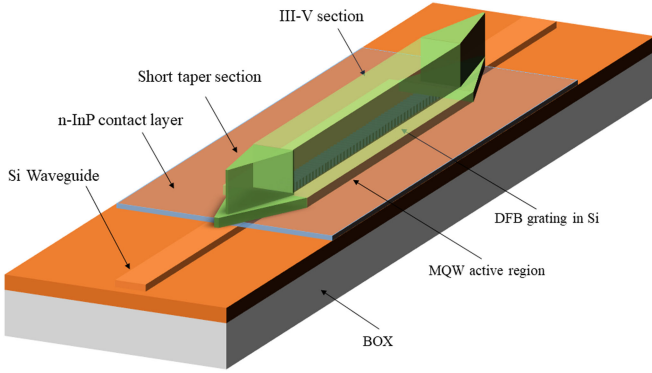


Fig. 1. Schematic structure of the heterogeneously integrated DFB laser diode on the Si waveguide.

In this paper, we demonstrate a high-efficiency, short-cavity heterogeneously integrated C-band DFB laser on a Si waveguide realized using adhesive bonding. In the coming sections, we first discuss the simulation results regarding the integrated cavity design. Then the fabrication technology is explained. After that the experimental results of the fabricated device are presented. The static characteristics of the device operating in the C-band show single mode behavior with a side mode suppression ratio (SMSR) up to 44 dB and a wall-plug efficiency up to 13% at 20 °C. In addition, the dynamic response is described by measuring the small signal modulation response followed by a data transmission experiment at 20 Gb/s over a 2 km long, single mode fiber. Finally, the paper ends with a conclusion.

II. DESIGN AND FABRICATION

A. Short Integrated Cavity Design

Fig. 1 shows the simplified schematic of the heterogeneously integrated DFB laser on a pre-patterned SOI circuit. The SOI platform consists of a 400 nm thick Si device layer on a 2 μm buried oxide (BOX) layer. The 200 μm long cavity is determined by a 1 μm wide, first order, quarter-wave shifted grating in the Si with a 60 nm etch depth. The 60 nm etched Si waveguide is then connected to a 180 nm etched Si waveguide in which the 180 nm etched grating couplers are incorporated. In the III-V section, the epitaxial layer stack consists of a 200 nm thick highly-doped p-InGaAs contact layer, a 1.5 μm thick p-InP cladding layer, an InGaAsP multi-quantum well (MQW) active region with 6 quantum wells surrounded by 100 nm thick separate confinement heterostructure (SCH) layers, and a n-InP

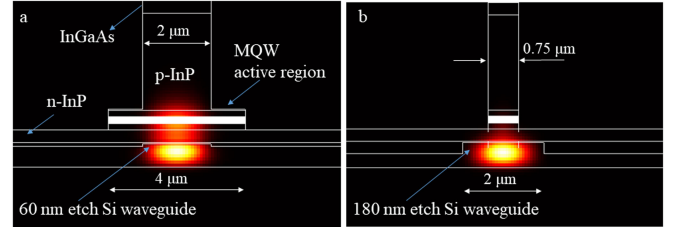


Fig. 2. Optical mode profile in the III-V/Si cross-section. (a) Mode profile in the laser cross-section. (b) Mode profile at the III-V taper tip.

contact layer with a thickness of 190 nm. The laser mesa is 2 μm wide and consists of two short spot-size converters at the ends.

As we discussed in the previous section, the key element in designing an integrated III-V-on-SOI cavity is to accurately analyze the optical mode profile in the III-V/Si cross-section. In order to make a short cavity, the mode has to be sufficiently confined to the active region to provide sufficient gain for lasing. On the other hand, as the optical mode is more confined in the Si waveguide underneath, it will experience lower optical absorption loss since there are no doped layers in the Si device. In addition, the impact of the sidewall scattering loss also decreases. The hybrid optical mode profile is shown in Fig. 2(a). As can be seen, the optical mode is more confined to the Si waveguide. The simulated confinement factor in the MQW active region is about 4% and the effective index of the fundamental mode is 3.2480. The DFB grating period Λ is then estimated by [20]:

$$\Lambda = \lambda_g / 2n_{eff} \quad (1)$$

where λ_g is the Bragg wavelength (1550 nm) and n_{eff} denotes the effective index of the fundamental optical mode in the cavity. In this structure, we designed the MQW active region to be wider than the III-V mesa in order to reduce surface recombination and decrease the effect of the sidewall scattering loss caused by the etching of the active region. In addition, in order to suppress the oscillation of higher order transverse modes in the cavity, the Bragg grating is etched only in the center of the silicon waveguide. The alternative approach to have single mode operation is via proton implantation to define a current channel in a wide III-V mesa [17], [21]. Finally, as Fig. 2(b) depicts, the optical mode profile at the short taper tip is predominantly in the Si waveguide. This design enables the efficient coupling of the light from the III-V/Si laser into the Si waveguide circuit just by incorporating a 10 μm long taper.

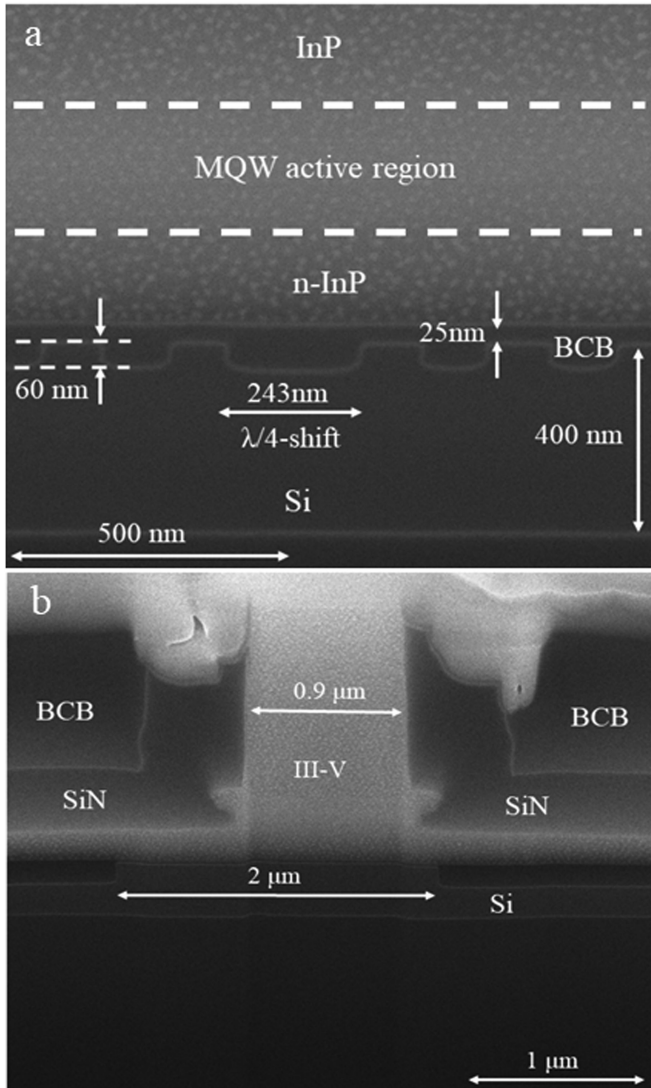


Fig. 3. FIB cross-section of the fabricated device. (a) Longitudinal cross-section of the laser. (b) Transversal cross-section close to the taper tip.

B. Device Fabrication

The SOI circuit is fabricated by a Voyager electron beam lithography (EBL) system. First, the shallow-etched waveguide and first order grating are patterned. Fig. 3 shows the focused ion beam (FIB) longitudinal cross-section image of the fabricated device. The quarter wave shift grating with a grating period of 243 nm is depicted beneath the bonded III-V material. The cavity length determined by the 60 nm etch-depth quarter-wave shifted DFB grating section is 200 μm . In a second etch step, a 180 nm deep Si waveguide is defined by writing 5 μm trenches at the sides, together with the fiber-to-chip grating couplers.

After the preparation of the SOI circuit, the III-V epitaxial layer is bonded upside-down onto the SOI waveguide wafer using an adhesive bonding approach. A 25 nm thick divinyl-bis-benzocyclobutene (DVS-BCB) is used as an adhesive bonding layer in this fabrication. After completion of the bonding, the InP substrate is removed by a selective wet etching process in HCl. The laser processing starts with the deposition of a 200

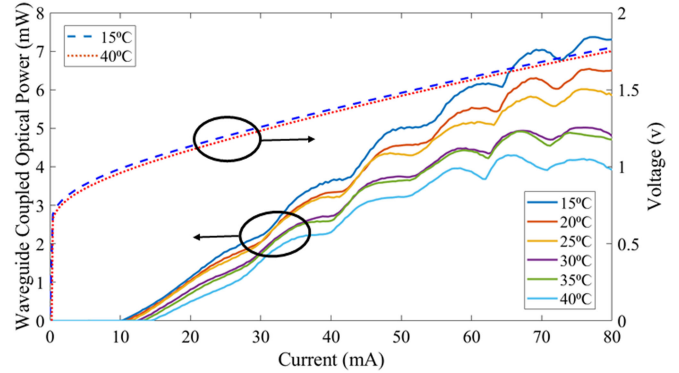


Fig. 4. Waveguide-coupled optical output power (single-sided) versus DC bias current (left), and I-V curves (right) at various operating temperatures.

nm thin SiN layer as a hard mask for the mesa definition using i-line optical lithography. The mesa is created by etching the SiN by means of a reactive ion etching (RIE) tool as well as etching of the InGaAs contact layer and InP cladding layer using inductively coupled plasma (ICP). Unlike in our previous fabrications [11], [22], we avoid using wet etching of the InP cladding in HCl to make a V-shaped mesa. Instead, we etch down the whole InP layer with ICP which results in lower sidewall roughness compared to the case where we use HCl for etching the mesa. Fig. 3(b) depicts the cross-section image of the fabricated device at the taper section. After this step, we again deposit SiN not only to protect the side-wall of the mesa but also to use it as a second hard mask for making a wide active region. The active region is etched using mostly ICP etch followed by a short selective wet etch with a $\text{H}_2\text{O}:\text{H}_3\text{PO}_4:\text{H}_2\text{O}_2$ solution. Afterwards, another optical lithography is carried out to deposit the Ni/Ge/Au/Ti n-contact. Subsequently, the device is passivated with SiN and BCB before depositing the Ti/Au p-contact with the same process. Finally, GSG pads with a pitch of 100 μm are created to enable the static and dynamic characterizations.

III. STATIC CHARACTERISTICS

The static characterization of the DFB lasers is done by placing the fabricated chip on a temperature-controlled stage. The laser is biased with a Keithley 2400 current source and the laser emission is collected through a standard single mode fiber coupled to the on-chip grating coupler structures. The coupling efficiency of the grating couplers is determined by the separate reference structures on the chip and a 10 dB fiber-to-chip loss is measured at 1563 nm.

The DFB laser L-I curve is measured at different stage temperatures and the results are depicted in Fig. 4. The measured threshold current at 20 $^\circ\text{C}$ is 10.5 mA and it increases up to 14.5 mA by increasing the operating temperature to 40 $^\circ\text{C}$. A waveguide-coupled optical power up to 6.5 mW is obtained from a single facet. Due to the symmetrical configuration, the same results are obtained from the other output of the laser. In addition, the measured I-V curve in Fig. 4 shows that the voltage remains below 2 V over operating temperatures. As it can be seen, there

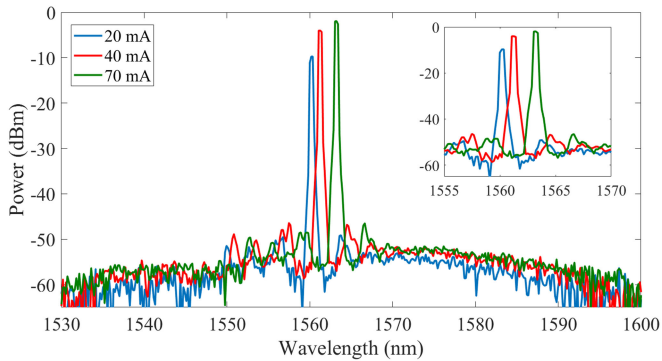


Fig. 5. Optical spectrum at 20 °C at various bias currents. 3 nm redshift in the lasing mode is observed by increasing the bias current from 20 mA to 70 mA and the corresponding SMSR improves from 39 dB to 44 dB. The inset represents a closer look at the lasing wavelengths.

are ripples or kinks in the L-I curves due to the reflections from the grating coupler. The phase of these reflections changes with current due to the heating of the device.

Fig. 5 illustrates the optical spectrum for various bias currents at 20 °C. The laser operates at 1560 nm at a bias current of 20 mA and shifts to 1561 nm and 1563 nm as the current increases to 40 mA and 70 mA, respectively. Stable optical lines with no hopping in the lasing wavelength are observed at 40 mA and 70 mA which are close to the kinks in the L-I curve. A SMSR of about 44 dB is obtained at 70 mA of bias current and the measured stop band width is 4 nm, which corresponds with $\kappa L = 1$ for the 200 μm long cavity. Assuming a thermal dependence of the effective index of $2 \times 10^{-4}/\text{K}$ [23], the shift of the laser wavelength with the increased current corresponds with a heating by 30K when the current is increased from 20 to 70mA. The wall-plug efficiency of the laser as a function of the bias current at different operating temperatures is shown in Fig. 6(a). As can be seen, more than 12% wall-plug efficiency is achievable at room temperature. For a better understanding of the device performance, in Fig. 6(b) the wall-plug efficiency is plotted versus total optical output power collected from both output facets. At the semi-cooled operation (40 °C), up to 9% wall-plug efficiency is measured.

IV. DYNAMIC CHARACTERISTICS

Small-signal measurements were carried out using an Agilent N5247A vector network analyzer (VNA) to provide radio frequency (RF) electrical signals. Using a bias tee, the RF signal is combined with a DC bias current to modulate the laser by means of a Cascade Infinity GSG RF probe with 100 μm pitch. Then, the laser light is sent to a Discovery DSC-10H photodetector (PD) with a bandwidth of 43 GHz and the output electrical signal is sent back to the VNA to measure the small signal S parameters. Fig. 7 depicts the small signal S_{21} parameter, measured at room temperature at various bias currents. At a bias current of 60 mA the modulation bandwidth of the device is found to be around 15 GHz. The main limiting factor of the modulation bandwidth in our design (and the similar ones) is the confinement factor of the optical mode in the MQW active region. As we mentioned

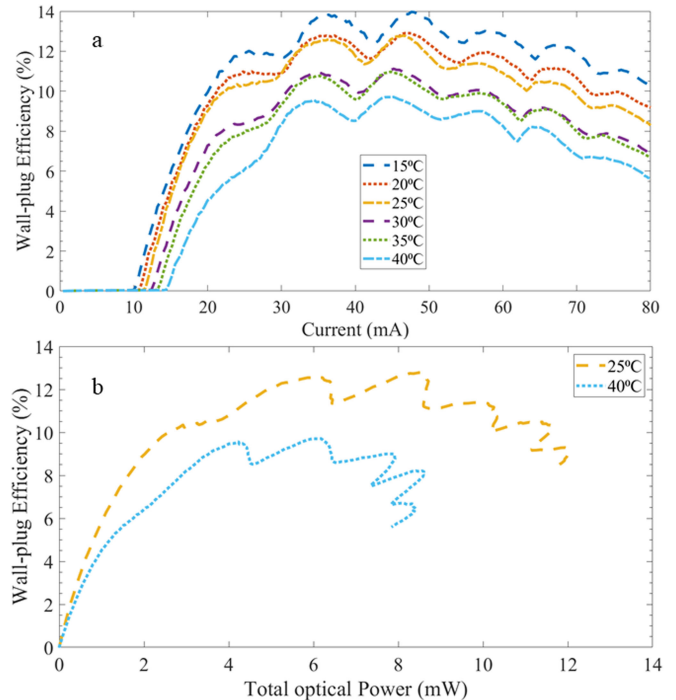


Fig. 6. Wall-plug efficiency illustration for the 200 μm long cavity DFB laser on SOI. (a) Wall-plug efficiency versus bias current at various operating temperatures and (b) wall-plug efficiency as a function of total output power at 25 °C and semi-cooled operation (40 °C).

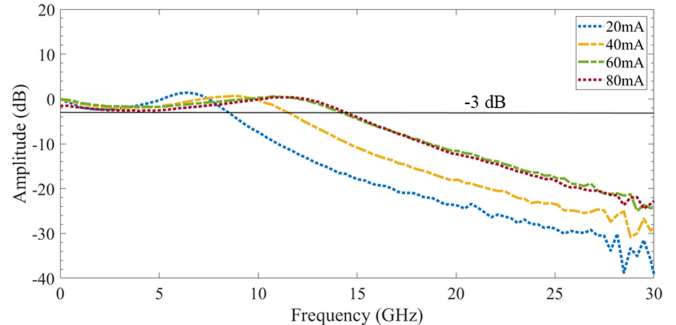


Fig. 7. Small signal modulation characteristics at various bias currents.

earlier, the optical mode in this design is mostly confined in the Si waveguide. This can be beneficial in decreasing optical loss and increasing the internal efficiency, whereas the consequence is the degradation of the modulation bandwidth.

The large signal intensity modulation of the laser is investigated by carrying out a data transmission experiment. Fig. 8 describes the block diagram of the setup used for this measurement. The modulation signal is generated using a Keysight M8196A arbitrary waveform generator (AWG). An SHF807 RF amplifier is used to amplify the output signal of the AWG. Then, the amplified modulation signal is combined with a DC current via a bias tee and the corresponding output signal drives the laser by using the GSG RF probe. The laser optical output signal is directly sent to the photodetector, of which the output is fed to a Keysight 70 GHz sampling oscilloscope without using any

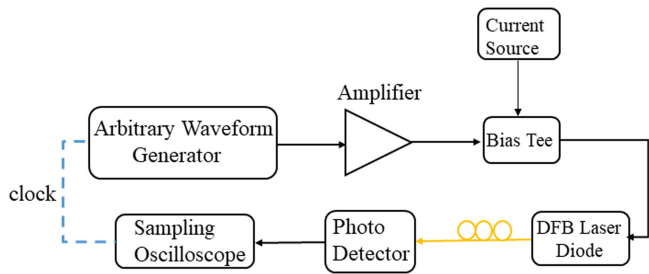


Fig. 8. Block diagram of the experimental setup for the data transmission.

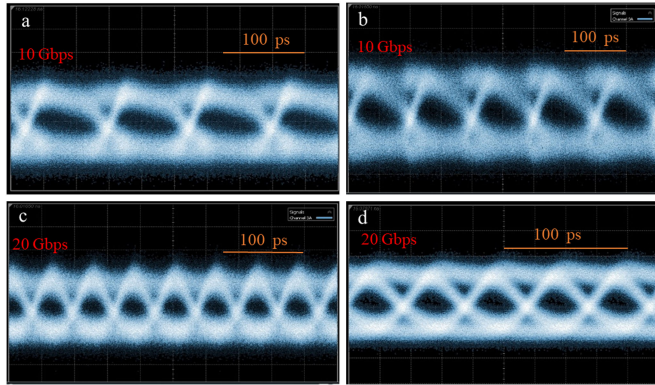


Fig. 9. Data transmission experiment; (a) and (c) eye diagram for back to back configuration at 10 Gb/s and 20 Gb/s, respectively. (b) and (d) eye diagram after transmission over a 2 km fiber at 10 Gb/s and 20 Gb/s, respectively.

RF amplifiers. The large signal characterization results are illustrated as eye diagrams in Fig. 9. Non-return-to-zero (NRZ) data transmission with a Pseudo-Random-Binary-Sequence (PRBS) pattern length of 2^7-1 are verified. Open eyes can be observed at 10 Gb/s and 20 Gb/s after transmission over a 2 km long non-zero dispersion-shifted-fiber (NZ-DSF). A 4 dB extinction ratio is obtained at 20 Gb/s. These results are achieved at a bias current of 70 mA without using any optical or electrical amplifiers at the receiver, nor equalization.

V. CONCLUSION

We discussed the design, fabrication and static and dynamic characterization of high-efficiency, short-cavity DFB laser diodes, heterogeneously integrated on SOI, based on adhesive bonding. In order to decrease the optical loss inside the cavity, we designed a configuration where the optical mode inside the laser cavity is predominantly confined to the Si waveguide underneath. In the static characterization of the fabricated DFB laser diode, the experimental results show above 12% wall plug efficiency at 25 °C. In addition, stable single mode operation with a SMSR up to 44 dB is achieved. We also reported the dynamic characteristics of the laser diode by measuring the small-signal and large-signal modulation responses. Up to 15 GHz modulation bandwidth is obtained at the bias current of 60 mA. The data transmission experiment with NRZ modulation depicts open eye diagrams up to 20 Gb/s without using any equalization. The same design concept can also be applied to O-band lasers to serve the datacom market.

ACKNOWLEDGMENT

J. Rahimi would like to thank M. Muneeb for supporting in preparation of the SOI circuit using EBL and L. V. Landschoot for FIB images.

REFERENCES

- [1] S. Matsuo and T. Kakitsuka, "Low-operating-energy directly modulated lasers for short-distance optical interconnects," *Adv. Opt. Photon.*, vol. 10, no. 3, pp. 567–643, 2018, doi: [10.1364/aop.10.000567](https://doi.org/10.1364/aop.10.000567).
- [2] L. Chen *et al.*, "Silicon photonics in optical coherent systems," in *Proc. 23rd Opto-Electron. Commun. Conf.*, 2018, pp. 1–2, doi: [10.1109/OECC.2018.8730067](https://doi.org/10.1109/OECC.2018.8730067).
- [3] A. W. Fang *et al.*, "Electrically pumped hybrid algalinas-silicon evanescent laser," *Opt. Exp.*, vol. 14, no. 20, 2006, Art. no. 9203, doi: [10.1364/oe.14.009203](https://doi.org/10.1364/oe.14.009203).
- [4] J. Zhang *et al.*, "III-V-on-Si photonic integrated circuits realized using micro-transfer-printing," *APL Photon.*, vol. 4, no. 11, 2019, Art. no. 110803, doi: [10.1063/1.5120004](https://doi.org/10.1063/1.5120004).
- [5] D. Liang and J. E. Bowers, "Recent progress in heterogeneous III-V-on-silicon photonic integration," *Light Adv. Manuf.*, vol. 2, no. 1, pp. 1–25, 2021, doi: [10.37188/lam.2021.005](https://doi.org/10.37188/lam.2021.005).
- [6] D. J. Blumenthal, "Photonic integration for UV to IR applications," *APL Photon.*, vol. 5, no. 2, 2020, doi: [10.1063/1.5131683](https://doi.org/10.1063/1.5131683).
- [7] A. Malik *et al.*, "Low noise, tunable silicon photonic lasers," *Appl. Phys. Rev.*, vol. 8, no. 3, 2021, Art. no. 031306, doi: [10.1063/5.0046183](https://doi.org/10.1063/5.0046183).
- [8] A. R. Adams, M. Asada, Y. Suematsu, and S. Arai, "The temperature dependence of the efficiency and threshold current of $\text{In}_{1-x}\text{Ga}_x\text{AsyP}_{1-y}$ lasers related to intervalence band absorption," *Jpn. J. Appl. Phys.*, vol. 19, no. 10, pp. L621–L624, 1980, doi: [10.1143/JJAP.19.L621](https://doi.org/10.1143/JJAP.19.L621).
- [9] I. P. Marko *et al.*, "Optical gain in GaAsBi/GaAs quantum well diode lasers," *Sci. Rep.*, vol. 6, pp. 1–10, 2016, doi: [10.1038/srep28863](https://doi.org/10.1038/srep28863).
- [10] S. Keyvaninia *et al.*, "Heterogeneously integrated III-V/silicon distributed feedback lasers," *Opt. Lett.*, vol. 38, no. 24, 2013, Art. no. 5434, doi: [10.1364/ol.38.005434](https://doi.org/10.1364/ol.38.005434).
- [11] A. Abbasi *et al.*, "Direct and electroabsorption modulation of a III-V-on-silicon DFB laser at 56 Gb/s," *IEEE J. Sel. Top. Quantum Electron.*, vol. 23, no. 6, pp. 1–17, Nov./Dec. 2017, doi: [10.1109/JSTQE.2017.2708606](https://doi.org/10.1109/JSTQE.2017.2708606).
- [12] M. Shahin *et al.*, "80-Gbps NRZ-OOK electro-absorption modulation of InP-on-Si DFB laser diodes," *IEEE Photon. Technol. Lett.*, vol. 31, no. 7, pp. 533–536, Apr. 2019, doi: [10.1109/LPT.2019.2900518](https://doi.org/10.1109/LPT.2019.2900518).
- [13] C. Zhang, S. Zhang, J. D. Peters, and J. E. Bowers, "8 × 8 × 40 gbps fully integrated silicon photonic network on chip," *Optica*, vol. 3, no. 7, pp. 785–786, 2016, doi: [10.1364/optica.3.000785](https://doi.org/10.1364/optica.3.000785).
- [14] C. Zhang *et al.*, "Low threshold and high speed short cavity distributed feedback hybrid silicon lasers," *Opt. Exp.*, vol. 22, no. 9, p. 10202, 2014, doi: [10.1364/oe.22.010202](https://doi.org/10.1364/oe.22.010202).
- [15] A. Gallet *et al.*, "Hybrid III-V on silicon integrated distributed feedback laser and ring resonator for 25 Gb/s future access networks," *J. Light. Technol.*, vol. 36, no. 8, pp. 1498–1502, 2018, doi: [10.1109/JLT.2017.2782012](https://doi.org/10.1109/JLT.2017.2782012).
- [16] R. Jones *et al.*, "Heterogeneously integrated InP/Silicon modulators: Fabricating fully functional transceivers," *IEEE Nanotechnol. Mag.*, vol. 13, no. 2, pp. 17–26, Apr. 2019, doi: [10.1109/MNANO.2019.2891369](https://doi.org/10.1109/MNANO.2019.2891369).
- [17] S. Matsuo *et al.*, "Directly modulated buried heterostructure DFB laser on SiO₂/Si substrate fabricated by regrowth of InP using bonded active layer," *Opt. Exp.*, vol. 22, no. 10, pp. 12139–12147, 2014, doi: [10.1364/oe.22.012139](https://doi.org/10.1364/oe.22.012139).
- [18] S. Yamaoka *et al.*, "Directly modulated membrane lasers with 108 GHz bandwidth on a high-thermal-conductivity silicon carbide substrate," *Nat. Photon.*, vol. 15, no. 1, pp. 28–35, 2021, doi: [10.1038/s41566-020-00700-y](https://doi.org/10.1038/s41566-020-00700-y).
- [19] N. P. Diamantopoulos *et al.*, "47.5 GHz Membrane-Iii-V-on-Si directly modulated laser for Sub-Pj/Bit 100-Gbps transmission," *Photonics*, vol. 8, no. 2, pp. 1–11, 2021, doi: [10.3390/photonics8020031](https://doi.org/10.3390/photonics8020031).
- [20] G. P. Agrawal and A. H. Bobeck, "Modeling of distributed feedback semiconductor lasers with axially-varying parameters," *IEEE J. Quantum Electron.*, vol. 24, no. 12, pp. 2407–2414, 1988, doi: [10.1109/3.14370](https://doi.org/10.1109/3.14370).
- [21] T. Komljenovic *et al.*, "Heterogeneous silicon photonic integrated circuits," *J. Light. Technol.*, vol. 34, no. 1, pp. 20–35, 2016, doi: [10.1109/JLT.2015.2465382](https://doi.org/10.1109/JLT.2015.2465382).
- [22] B. Haq *et al.*, "Micro-transfer-printed III-V-on-silicon C-band distributed feedback lasers," *Opt. Exp.*, vol. 28, no. 22, pp. 32793–32801, 2020.

- [23] E. Gini and H. Melchior, "Thermal dependence of the refractive index of InP measured with integrated optical demultiplexer," *J. Appl. Phys.*, vol. 79, no. 8, pp. 4335–4337, 1996, doi: [10.1063/1.361742](https://doi.org/10.1063/1.361742).

Javad Rahimi received the bachelor's degree in electrical engineering from the Tabriz University, Tabriz, Iran, and the master's degree in electronics engineering from the Tarbiat modares Univerity, Tehran, Iran, in 2015. He was a Research Fellow with the Politecnico di Torino, Turin, Italy during 2016–2017, working on single section comb semiconductor lasers. In 2018, he joined the Photonics Research Group, with the Ghent University where he is currently working toward the Ph.D. degree on heterogeneous integration of III-V-on-Si lasers for telecommunication applications.

Joris Van Kerrebrouck was born in Ghent, Belgium, in 1989. He received the M.Sc. and Ph.D. degrees in electrical engineering from Ghent University, Ghent, Belgium, in 2014 and 2020, respectively. He is currently a Postdoctoral Researcher with IDLab Design Group, Department of Information Technology (INTEC), Ghent University, Belgium. His research interests include radio-over-fiber, point-to-point optical links, and nonlinear electro-optical systems.

Bahawal Haq Graduated from Masdar Institute in the master's program in microsystems engineering. Afterwards, he completed Ph.D. degree from the Ghent University-IMEC in Photonics Engineering. He is currently working as a Sr. Integration Engineering with the Globalfoundries, Dresden, Germany. His research interests include micro-transfer-printing of III-V-on-Si devices and III-V-on-Si heterogenous integration.

Johan Bauwelinck (Senior Member, IEEE) received the Ph.D. degree in applied sciences and electronics from the Ghent University, Ghent, Belgium, in 2005. Since October 2009, he has been a Professor with the INTEC Department, Ghent University, and since 2014, he has been Leading the Internet Technology and Data Science Lab Design Group. He has promoted 18 Ph.D.s and coauthored more than 150 publications and ten patents in the field of high-speed electronics and fiber-optic communication. He was and is active in the EU-funded projects GIANT, POWERNET, PIEMAN, EuroFOS, C3- PO, Mirage, Phoxtrout, Spirit, Flex5Gware, Teraboard, Streams, and WIPE conducting research on advanced electronic integrated circuits for next generation transport, metro, access, data-center and radio-over-fiber networks. His research interests include high-speed, high-frequency (opto-) electronic circuits and systems, and their applications on chip and board level, including transmitter and receiver analog front-ends for wireless, wired and fiber-optic communication or instrumentation systems. He is a member of the ECOC Technical Program Committee.

Gunther Roelkens (Senior Member, IEEE) received the degree in electrical engineering from Ghent University, Ghent, Belgium, in 2002, and the Ph.D. degree from the Department of Information Technology (INTEC), Ghent University, Ghent, Belgium, in 2007. He is currently a Full Professor with Ghent University. In 2008, he was a Visiting Scientist with IBM TJ Watson Research Center, New York, NY, USA. His research interests include the heterogeneous integration of III–V semiconductors and other materials on top of silicon waveguide circuits and electronic/photonic co-integration. He was a holder of an ERC starting grant (MIRACLE), to start up research in the field of integrated mid-infrared photonic integrated circuits.

Geert Morthier (Senior Member, IEEE) received the degree in electrical engineering and the Ph.D. degree from Ghent University, Ghent, Belgium, in 1987 and 1991, respectively. Since 1991, he has been a member of the permanent staff of imec and since 2001 he is part-time Professor with Ghent University. He has authored or coauthored more than 200 papers in the field and holds several patents. He is also one of the two authors of the Handbook of Distributed Feedback Laser (Artech House, 1997). His main interests include the modeling and characterization of optoelectronic components. From 1998 to end of 1999, he was the Project Manager of the ACTS Project ACTUAL dealing with the control of widely tunable laser diodes, from 2001 to 2005, he was the Project Manager of the IST Project NEWTON on new widely tunable lasers, and from 2008 to 2011, he was the Project Manager of the FP7 Project HISTORIC on microdisk lasers.